Irradiation Effects in Ultrathin Si/SiO_2 Structures

J.L. Cantin[1], H.J. von Bardeleben[1] and J.L. Autran[2]

[1]Groupe de Physique des Solides, UMR CNRS 75-88, Universités Paris 6 & 7, 2 Place Jussieu, F-75251 Paris
[2]Laboratoire de Physique de la Matière, UMR CNRS 5511, INSA de Lyon, Bat. 502, F-69621 Villeurbanne Cedex

Abstract

The total dose response of Si/SiO_2 structures with ultrathin (20-40 Å) thermal oxide layers grown on porous silicon substrates has been studied by Electron Paramagnetic Resonance (EPR) spectroscopy. The modification of the interface defect passivation and the generation of oxide defects have been analysed as a function of dose for three series of samples with different initial hydrogen passivation states.

I. INTRODUCTION

The behaviour of Si/SiO_2 structures exposed to high energy irradiation (x-ray, γ) has been extensively studied in the past [1]. Most of these studies were motivated by the technological importance of the Si/SiO_2 system in metal-oxide-semiconductor (MOS) devices and have therefore been focused on the modification of the electrical characteristics of the irradiated devices. In general, irradiation generates and modifies point defects in the oxide and affects the passivation state of interface defects. In addition more subtle effects such as latent interface trap generation after radiation or radiation-induced charge relaxation have been evidenced. The basic processes involved are not yet fully understood, but it has become clear, that one key parameter for the modification of the electrically active defects in MOS structures is their hydrogen content [2].

As electrical measurements give no insight in the microscopic structure of the defects (an information necessary for the modelling of the irradiation effects), additional techniques and in particular Electron Paramagnetic Resonance (EPR) spectroscopy have been applied successfully [3]. The main defects assessed were the E' centre (positively charged oxygen vacancy) and the different P_b centres localised at the Si/SiO_2 interface [4-5]. The latter ones are electrically active and thus connected with the interface traps probed by electrical techniques. Two types of P_b centres with different microscopic structures have been evidenced: the P_{b0} centres, which are $\bullet SiSi_3$ silicon dangling bond defects oriented along the [111] direction (they occur at the (111) but also at the (001) and (110) Si/SiO_2 interfaces) and the P_{b1} centres, which are specific of the (001) interface [5,6]. For the P_{b1} centre, the model of a Si-Si dimer has been put forward [7]. As the reconstruction by dimer formation is a characteristic of the (100) interface, the existence of such a defect is not too surprising. Both P_{b0} and P_{b1} defects can be thermally passivated by molecular hydrogen with similar activation energies [8].

Previous EPR studies were mainly performed on thick SiO_2 layers, typically with oxide thickness in the range 10 to 100 nm. It is a priori not evident, that similar results will be obtained for ultrathin oxides (< 5 nm), which are now actively studied for future generation of MOS devices. In this paper, we report a preliminary EPR study of x-ray irradiation effects in ultrathin Si/SiO_2 structures with oxide layer thicknesses in the range 20-40 Å.

From the experimental point of view, the study of such ultrathin layers by EPR is difficult (if not impossible) due to sensitivity reasons: the standard EPR technique is indeed limited to $\sim 10^{10}$ spins (for 1 G linewidth). which corresponds in the case of an ultrathin layer to a defect density of about 10^{18} $cm^{-3}$to allow their detection. To overcome this difficulty we have chosen to grow the oxide layers on porous silicon substrates. Such a material offers a high intrinsic surface area (~200 m^2/cm^3) which allows us to detect and quantify paramagnetic defects under highly improved conditions [9,10]. We have recently shown that the thermal oxide growth on porous Si proceeds with very similar kinetics as those obtained on bulk Si samples and gives rise to identical interface defects , which justifies their use as model substrate [11].

II. EXPERIMENTAL

The porous silicon has been obtained by electrochemical dissolution in HF/Ethanol electrolytes of boron-doped (100) Si substrates. Porous layers of typical ~10 μm thickness and ~60 % porosity have been prepared. The specific surface of 200 m^2/cm^3 multiplies in this case the external surface by a factor of 2×10^3. The entire set of samples originated from the same substrate; they were furnace oxidised at 1000 °C under 12 mbar of dry oxygen for 2 and 20 minutes respectively, which leads to the formation of 20 and 40 Å thick oxide layers. The oxide layer thickness was determined by correlated gas adsorption (BET), SIMS and nuclear reaction analysis experiments. In order to assess the influence of the H concentration on the defect evolution with total dose, we have studied three different sets of samples : as oxidised, vacuum annealed and forming gas passivated samples. In the first set (named AsOx), one can assume an intermediate H content, set by the residual hydrogen content of the furnace. The second set of samples (labelled DP) has been submitted to a depassivating treatment at 650 °C under vacuum (< 5×10^{-7} Torr) for 60 minutes [12]. The last set of samples (FG) has been treated in forming gas at 450 °C for 40 minutes in order to fully passivate the interface defects.

0018-9499/98$10.00

The samples were irradiated without electrical bias at room temperature with doses ranging from 50krad up to 200 Mrad(SiO_2) using an Aracor model 4100 (10 keV x-rays) and with a dose rate of 10 krad (SiO_2) / s.

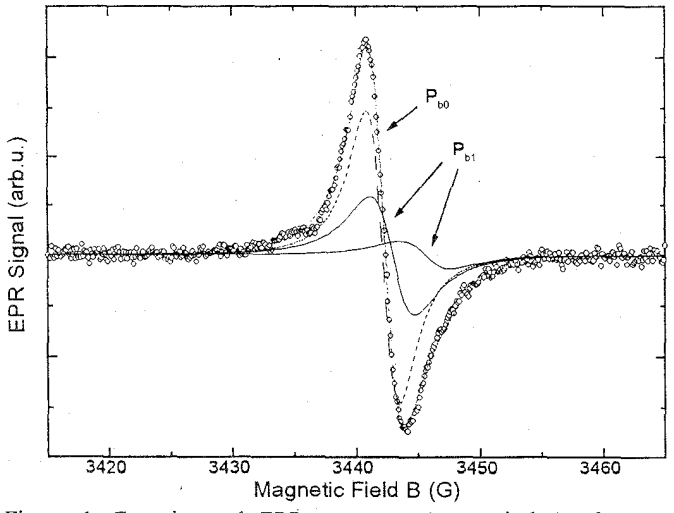

Figure 1. Experimental EPR spectrum (open circles) of an as oxidised Si/SiO2(40Å) sample measured at room temperature for a magnetic field orientation B//[001]. The total spectrum is decomposed in the respective contributions of the P_{b0} and P_{b1} centres (dashed and full lines).

All the samples were analysed a few days after irradiation; additional test measurements, taken some weeks later, gave no indication for any charge relaxations. The EPR experiments were performed at room temperature using an X-band spectrometer. For the determination of the g-factors of the defects, the microwave frequency was measured using a frequency counter and the magnetic field was determined with a NMR probe. The absolute spin numbers were obtained by comparison with a ruby reference sample.

III. EPR Results

Fig. 1 shows a typical EPR spectrum of a porous Si/SiO_2 structure with a 40 Å thick oxide layer in the as oxidised state. Even though the spectrum is only shown for BII[001], the decomposition is based on the analysis of the complete angular variation of the EPR spectrum for a rotation of the magnetic field in the (110) plane; from this we deduce, that the total spectrum is the superposition of two different spectra, which from their g tensor can be attributed to the two interface defects, P_{b0} and P_{b1}; no oxide related defect is observed before irradiation. The EPR spectrum of the P_{b1} defect contains one additional line for B//[001] as compared to the « usual » EPR spectra known from (100)Si/SiO_2 bulk samples. This is due to the fact that in porous Si in addition to the external (100) plane, the other (010) and (001) planes are equally present due to its three-dimensional structure. The EPR parameters of the P_b centres are not modified by the reduction in the oxide thickness [6].The defect concentrations of P_{b0} and P_{b1} in this sample are $\sim 10^{12}$ cm^{-2} After vacuum annealing or forming gas treatment, the concentrations of the interface defects are typically increased by 30 % or decreased by 70 % respectively. The FG treatment is found to passivate both interface defects P_{b0} and P_{b1} in the same way, in agreement with a recent study by Stesmans [8].

A. Global Evolution of the EPR Spectra as a Function of Total Dose

Fig. 2 shows the evolution with total dose of the EPR spectra in the FG annealed 40 Å samples. We observe the increase of the initially low P_b centre concentration as well as the emergence of two additional isotropic EPR spectra. The

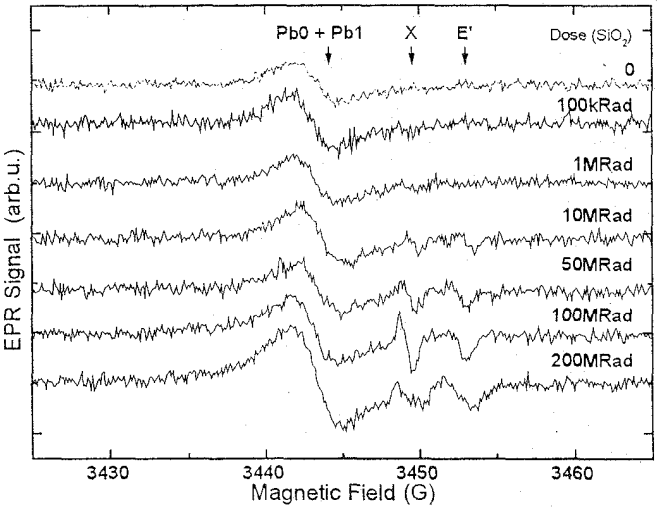

Figure 2. Evolution of the total EPR spectra with total dose for a series of 40 Å thick FG annealed samples. The EPR spectra, shown for B//[001], are optimised for the observation of the Pb centres, leading here to an artificial broadening of the X and E' spectra.

intensity of the different spectra increases monotonously with total dose in the whole total dose range. The two isotropic spectra are related to oxide defects. The first one (labelled X) is characterised by a g-factor of g = 2.0027 and a linewidth of ΔB_{pp} = 0.8 G. This spectrum is probably due to a carbon contamination induced carbon dangling bond defect ; it does not correspond to the EX centre, as no hyperfine structure is observed. The second EPR spectrum is identified by its g-tensor and particular lineshape as the E' centre. No E'_δ centres were detected at any stage of this study. These four defects (P_{b0}, P_{b1}, X, E') were observed in all sets of samples.

B. Evolution of Interface Defects with Irradiation Dose

1) Vacuum annealed layers

In the simple model of a complete depassivation of P_b centres induced by the vacuum annealing treatment and assuming that the annealing effect is only limited to the depassivation of P_b centres, no variation of their concentration with total dose is expected. Nevertheless, the experimental data of Fig. 3 clearly show, that the P_{b0} and P_{b1} centre concentrations vary with total dose up to 25 % for both oxide thickness. For the 40 Å samples, we observe an increase of the total P_b centre concentration (sum of P_{b0} and P_{b1}) with total dose up to 100 Mrad. The rate of this increase is $\sim 2\times 10^{11}$

$Mrad(SiO_2)^{-1}$ for the lowest doses and becomes lower (it is divided by a factor of ~3) in the linear regime between 10 and 100 Mrad. For the highest dose (200 Mrad), a decrease of the P_b centre concentration is finally observed. Concerning the 20 Å layers, the variations are inverted : from 0 to 100 Mrad, the P_b centre concentration decreases by ~20 % and, at this dose, both set of samples exhibit comparable P_b centre concentrations. For the highest dose (200 MRad), the concentration increases once again and becomes higher than the initial one. A more detailed analysis of these results shows that the initial (i.e. pre-rad) difference in the total P_b centre concentrations between the two series of samples is essentially

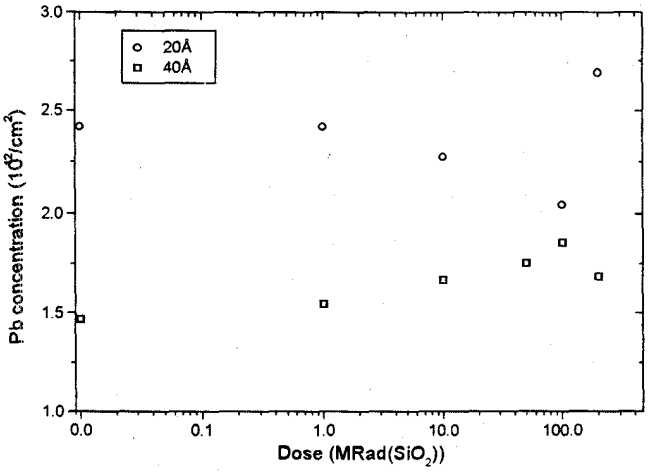

Figure 3: Total P_b centre concentration (P_{b0} + P_{b1}) as a function of total dose for vacuum annealed samples.

due to the P_{b1} centres, which have a higher concentration in the 20 Å samples than in the 40 Å ones. As far P_{b0} centres are concerned, their concentrations are equal in both types of layers. We observe for these vacuum annealed samples, that the initial P_{b0} to P_{b1} concentration ratio is not significantly modified by the irradiation.

2) FG annealed layers

In the FG annealed samples, we observe once again different behaviours with dose for the two layer thickness. As illustrated in Fig. 4, the 40 Å oxides show an increase in the total P_b centre concentration by a factor of ~2 for the lowest dose (100 kRad). In the next range, i.e. between 1 and 50 MRad, the concentration increases further by ~2. Finally, for the highest doses of 100 and 200 Mrad, the interface defect density increases again by a factor of ~2. For the 20 Å oxide layers, we observe no variation up to 300krad ; then a continuous increase up to the final dose of 200Mrad. In addition, the shape of the EPR spectrum changes and the decomposition of the global response in the respective P_{b0} and P_{b1} contributions shows, that only the P_{b0} centre concentration is increasing with the total dose, whereas P_{b1} remains constant. Nevertheless, the irradiation induced interface defect concentration in the 40 Å samples is low with only ~2×10^{11}cm^{-2} for a total dose of 100 Mrad. In Fig. 5 we compare the evolution of the total P_b centre concentration for

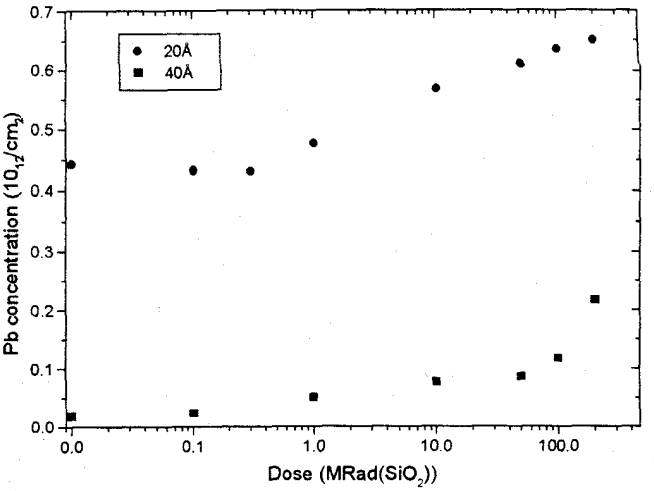

Figure 4: Total P_b centre concentration (P_{b0} + P_{b1}) as a function of total dose for FG annealed samples.

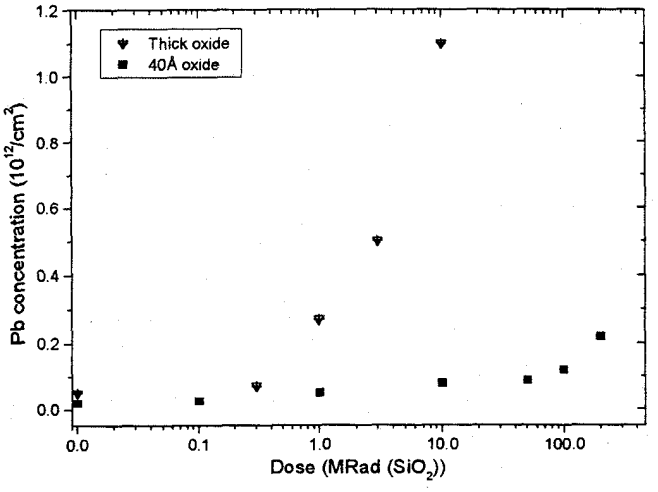

Figure 5: Comparison of the total P_b centre formation as a function of total dose for a 600Å thick oxide layer [13] and for a 40 Å thick oxide ultrathin layer .

the 40 Å thick oxide layer sample and a conventional 600 Å thick oxide layer (data taken from Ref. [13]. It is clear, that the ultrathin layer exhibits a much higher resistance to irradiation than the thick oxide in terms of radiation-induced interface defects.

3) As oxidised samples

Finally we present the results obtained for the evolution of the P_b centres in the as oxidised 40Å layers, where we have an intermediate degree of passivation before irradiation (Fig. 6). In the early stages of irradiation, we observe a weak increase in the P_b centre concentrations for doses up to 10 MRad similar to the vacuum annealed layer. Then for higher doses, the P_b centre concentration strongly decreases and approaches the value of the degraded FG passivated samples. This behaviour is similar to the total-dose response of DP samples observed at higher doses.

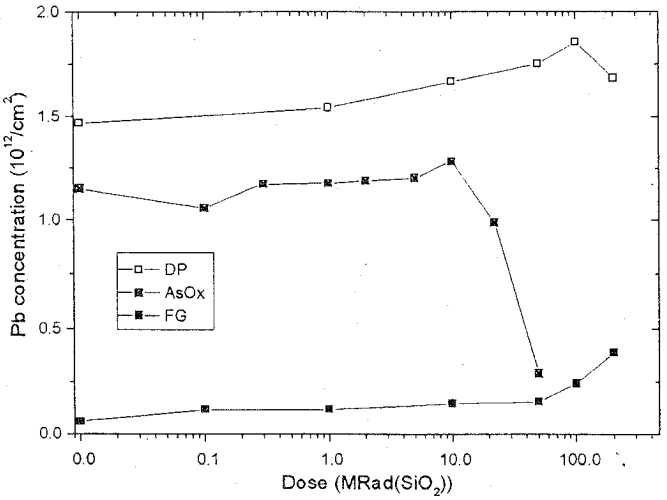

Figure 6: P_b centre concentration versus total dose for vacuum annealed (DP), as oxidised (AsOx) and forming gas annealed (FG) 40 Å layers.

C. *Evolution of Oxide Related Defects with Irradiation Dose*

In spite of the low oxide layer thickness of 20Å/40Å we have unambiguously identified in all irradiated samples the positively charged E' centre (Fig.2). The spin Hamiltonian parameters seem to be unchanged as compared to thick SiO_2 layers [10]. The particular lineshape of the E' centre spectrum demonstrates the amorphous character of the SiO_2 layer; clearly even for this small oxide thickness, the thermal SiO_2 does not present any indication for long range order.

Figure 7 shows the evolution of the E' centre concentration with total dose for the depassivated and passivated samples of both oxide thickness (20 and 40 Å). Whereas the area concentration (cm^{-2}) for a given dose is smaller for the 20 Å samples, very similar E' centre concentrations of ~1×10^{16} cm^{-3} for a total dose of 10 Mrad are detected in all type of samples after volume correction.

III. Discussion

Our results concerning the characterisation of oxide related defects allows us to emphasise two main tendencies : first, the E' center is induced by the irradiation with a similar rate in the 20 Å and 40 Å layers; second, the formation of paramagnetic E' centres is independent of the forming gas annealing treatment and thus of the configuration of the interface defects. This last observation would not be surprising for thick oxides, but for 20 Å oxides, it seems to indicate a direct E' centre formation process, not being the result of secondary reactions with diffusing radiation-induced species. Moreover, the formation rate of the E' centres does depend on total dose : in the initial stages, i.e. for total doses up to ~1MRad, the formation rate is at least three times higher than for the following doses. Similar observations have been reported by Kim et al. [14]. For total doses D between ~1Mrad and 200Mrad, we observe a constant $D^{0.5}$ dependence. Such power dependence seems typical for densified silica [15-16]. The analogy with densified SiO_2 is further confirmed by the absolute defect concentrations, which are in the range 2 to 8×10^{16} cm^{-3} [16].

As concerns the concentration changes of the P_b centres with total dose, their non monotonous character, the importance of the initial passivation and the thickness dependence do not allow us to propose any simple model. However, some basic observations can be formulated, which should be included in future models. The generation of positively charged oxygen vacancies in the oxide and the change in the interface passivation seem to be two completely uncorrelated processes.

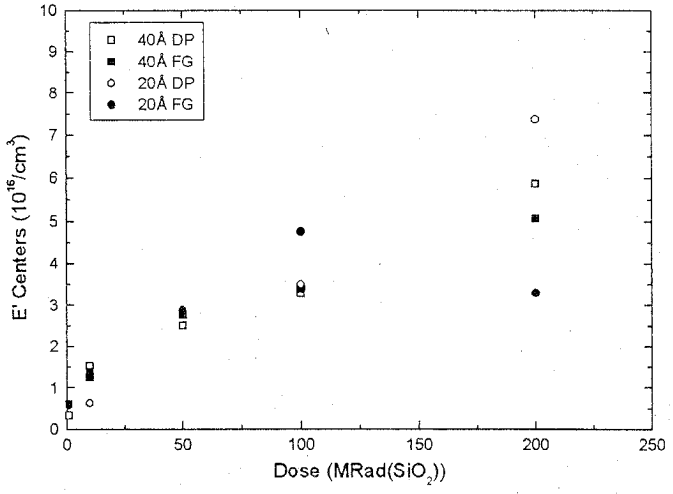

Figure 7. Volume concentration of paramagnetic E' centres versus total dose for DP and FG samples of both thickness.

As molecular hydrogen requires higher temperatures (typically above ~250 °C) for interaction with neutral P_b centres, the species interacting at room temperature must be atomic hydrogen. The observation of both passivating and depassivating actions- depending on the P_b centre passivation state -seems to indicate a dynamic equilibrium: $P_b + H \Leftrightarrow$ Si-H, which of course depends on the [H] concentration at the Si/SiO_2 interface. Whereas in thick oxides, the oxide layer should provide an infinite reservoir for radiolytic generation of atomic hydrogen, this is no longer the case for ultrathin oxide layers. The observed degradation of our FG annealed layers, which is attributed to the action of mobile atomic hydrogen, indicates, that this situation is not yet achieved in our samples; however, the role of the SiO_2/air interface, which might influence our results, must be studied in further experiments.

IV. Conclusion

In summary, our EPR study of x-ray irradiation induced defects in Si/SiO_2 structures with ultrathin oxide layers has qualitatively demonstrated the importance of the same paramagnetic defects as previously observed in thick (>100Å) oxide Si/SiO_2 structures: the P_{b0} and P_{b1} interface defects and the E' oxygen vacancy centre. The additional

radiation-induced paramagnetic defect, tentatively attributed to a carbon dangling bond defect, has not been reported previously.

Concerning the interface defects, our results show that the x-ray irradiation does not always lead to a generation of paramagnetic Pb centres, but that depending on the irradiation dose and the passivated fraction of the Pb centres an « annealing » can also occur. The FG annealed ultrathin samples show only a weak increase of the interface defect concentration, even for doses as high as 200 MRad. This increased radiation resistance is be attributed to the reduced hydrogen supply in ultrathin oxide layers.

ACKNOWLEDGEMENTS

The authors gratefully acknowledge their colleagues P. Paillet and J.L. Leray from the CEA (Bruyères-Le-Châtel) for part of the irradiations and helpful discussions.

REFERENCES

[1] D.L. Griscom, D.B. Brown, N.S. Saks, in *The Physics and Chemistry of SiO_2 and the Si/SiO_2 Interface -1*, edited by C.R. Helms and B. Deal (The Electrochem. Soc. Inc., Atlanta, 1988) p. 287.

[2] K.L. Brower, " Defects and impurities in thermal oxides on silicon, " Appl. Phys. Lett. 41, 251 (1982).

[3] J.F. Conley, in *The Physics and Chemistry of SiO_2 and the Si/SiO_2 Interface -3*, edited by H.Z. Massoud, E.H. Poindexter and C.R. Helms (The Electrochem. Soc. Inc., Los Angeles, 1996) p. 214.

[4] E.H. Poindexter, P.J. Caplan, " Characterisation of Si/SiO_2 interface defects by electron spin resonance, " Prog. Surf. Sci. 14, 201 (1983).

[5] E.H. Poindexter, " MOS interface states : overview and physicochemical-perspective " Semicond. Sci. Technol. 4, 961 (1989).

[6] J.L. Cantin, M. Schoisswohl, H.J. von Bardeleben, N. Zoubir, M. Vergnat, " An EPR study of the microscopic structure of the (100) Si/SiO_2 interface," Phys. Rev. B 52, 10599 (1993).

[7] A.H. Edwards in *The Physics and Chemistry of SiO_2 and the Si/SiO_2 Interface -1*, edited by C.R. Helms and B. Deal (The Electrochem. Soc. Inc., Atlanta, 1988) p. 271.

[8] A. Stesmans, " Comparative analysis of the H_2 passivation of interface defects at the (100)Si/SiO_2 interface using ESR ", Solid-State Commun. 97, 255 (1996).

[9] J.L. Cantin, M. Schoisswohl, H.J. von Bardeleben, V. Morrazzani, J.J. Ganem, I. Trimaille in *The Physics and Chemistry of SiO_2 and the Si/SiO_2 Interface -3*, edited by H.Z. Massoud, E.H. Poindexter, C.R. Helms (The Electrochem. Soc. Inc., Los Angeles, 1996) p. 28.

[10] J.L. Cantin, M. Schoisswohl, S. Lebib, H.J. von Bardeleben, A. Grosman, C. Ortega, "An Electron Paramagnetic Resonance Study of Defects in Ultrathin Si and SiGe Oxides ", French-Italian French Symposium on SiO_2, to be published (1997).

[11] V. Morrazzani, J.J. Ganem, J.L. Cantin in *Structural and Optical Properties of Porous Silicon Nanostructures*, edited by G. Amato, C. Delerue, H.J. von Bardeleben (Gordon&Breach), to be published (1997).

[12] J.H. Stathis, "Dissociation kinetics of hydrogen-passivated (100) Si/SiO_2 interface defects," J. Appl. Phys. 77, 6205 (1995).

[13] P.M. Lenahan et al, IEEE Trans. Nucl. Sci. NS28, 4105 (1981).

[14] Y.Y. Kim, P.M. Lenahan, " Electron Spin Resonance study of radiation induced paramagnetic defects in oxides grown on (100) silicon substrates ," J. Appl. Phys. 64, 3556 (1988).

[15] K. Awazu, K. Watanabe, H. Kawazoe, " Formation mechanisms of paramagnetic centers in Si/SiO_2 structures," Defect and Diffusion Forum 127-128, 1 (1995).

[16] R.A.B. Devine, J. Arndt, " Correlated defect creation and dose dependant radiation sensitivity in amorphous SiO_2, " Phys. Rev. B 39, 5132 (1989).

[1]